Available online at www.sciencedirect.com
ScienceDirect
Trans. Nonferrous Met. Soc. China 25(2015) 1986−1994
Transactions of Nonferrous Metals Society of China
www.tnmsc.cn

Effect of WS_2 addition on electrical sliding wear behaviors of Cu−graphite−WS_2 composites

Gang QIAN, Yi FENG, Yang-ming CHEN, Fei MO, Yu-qing WANG, Wen-hong LIU

School of Materials Science and Engineering, Hefei University of Technology, Hefei 230009, China

Received 4 June 2014; accepted 29 July 2014

Abstract: Four kinds of Cu-based composites with different mass ratios of graphite and WS_2 as lubricants were fabricated by hot-pressing method. Electrical sliding wear behaviors of the composites were investigated using a block-on-ring tribometer rubbing against Cu−5%Ag alloy ring. The results demonstrated that 800 °C was the optimum sintering temperature for Cu−graphite−WS_2 dual-lubricant composites to obtain the best comprehensive properties of mechanical strength and lubrication performance. Contact voltage drops of the Cu-based composites increased with increasing the mass ratio of WS_2 to graphite. The Cu-based composite with 20% graphite and 10% WS_2 showed the best wear resistance due to the excellent synergetic lubricating effect of graphite and WS_2. The reasonable addition of WS_2 into the Cu-graphite composite can remarkably improve the wear resistance without much rise of electrical energy loss which provides a novel principle of designing suitable sliding electrical contact materials for industrial applications.

Key words: Cu-based composites; graphite; WS_2; synergetic lubrication; wear rate; contact voltage drop

1 Introduction

As the critical component in electrical-rotor systems, sliding electrical contacts are used to conduct current between stationary part and moving part of motor or generator [1]. The wear of sliding electrical contact materials is the result of electro-thermo-mechanical multi-field coupling and it involves a number of damage processes such as abrasive and adhesive wear, erosive wear, oxidation wear, transfer film and structure modification [2−4]. Much effort has been devoted to studying the wear mechanism associated with sliding electrical contacts and the research results demonstrated that the current, pressure, humidity and velocity all have important influence on the wear of sliding electrical contact materials [5−9]. It is desirable for sliding electrical contact materials to operate with minimum mechanical loss, minimum electrical energy loss and long service life [10,11]. Self-lubricating composite materials are considered as the most efficient way to solve the problem of current collection and wear resistance [12−14].

Cu−graphite composites are extensively used as sliding electrical contact materials such as brushes and contact strips because of their superior combination of high mechanical strength, excellent electrical and thermal conductivities and self-lubricating nature [14−17]. However, with the rapid development of industries and advanced technologies, the conventional Cu−graphite composites are unable to meet the present requirements. It has been reported that when two or more solid lubricants are incorporated together, an unexpected synergetic lubricating effect can be observed, which is superior to the separate use of any one of the single lubricants [18,19]. HU et al [20] studied the synergistic effect of nano-MoS_2 and anatase nano-TiO_2 on the lubrication properties of MoS_2/TiO_2 nano-clusters and commented that the MoS_2/TiO_2 nano-clusters had significant advantages in friction reduction over pure nano-MoS_2. Doping MoS_2 with graphite can reduce its sensitivity to humidity and result in a synergistic lubricating effect in air [21,22]. The lubrication mechanism of WS_2 is similar to that of MoS_2 and it can provide an approximate 100 °C increase in maximum operating temperature and better lubricity compared with MoS_2 [23−25]. However, there are almost no reports about the research on the synergistic lubricating effect of

Foundation item: Projects (91026018; 60979017) supported by the National Natural Science Foundation of China; Project (20110111110015) supported by the Doctoral Fund of Ministry of Education of China
Corresponding author: Yi FENG; Tel: +86-551-62904715; E-mail: fyhfut@163.com
DOI: 10.1016/S1003-6326(15)63807-9

graphite and WS_2.

In the present work, Cu-based composites with different mass ratios of graphite and WS_2 as lubricants were prepared by hot-pressing method. Electrical sliding wear behaviors of the composites were tested using a block-on-ring tribometer rubbing against Cu−5%Ag alloy ring. The objective is to determine if graphite and WS_2 can result in a synergistic lubricating effect in electrical sliding wear.

2 Experimental

2.1 Materials preparation

Source powders were electrolytic copper powder (99.5% purity, 45 μm grain size), natural flake graphite (98.5% purity, 45 μm grain size) and WS_2 powder (99.9% purity, 45 μm grain size). The total amount of graphite and WS_2 in the Cu-based composites was fixed as 30% (mass fraction). The chemical compositions of the Cu-based composites are listed in Table 1. The four Cu-based composites used for this work were fabricated by powder metallurgy hot-pressing technique as follows: the powders of copper, graphite and WS_2 were mechanically mixed by OM−3SP04 planetary ball mill for 10 h. Then, the mixed powders were isothermally hot pressed by ZT−40−20Y vacuum-sintering furnace under pure argon atmosphere protection at 30 MPa for 1 h. The sintering temperatures were 900 °C for Cu−30G single-lubricant composite and 800 °C for the three Cu−G−WS_2 dual-lubricant composites, and the heating rate was 10 °C/min. The sintered composites were machined into rectangular blocks with dimensions of 24 mm × 20 mm × 8 mm for tribo-tests.

Table 1 Chemical compositions of Cu-based composites

Sample	w(Cu)/%	w(Graphite)/%	$w(WS_2)$/%
Cu−30G	70	30	0
Cu−25G−5WS_2	70	25	5
Cu−20G−10WS_2	70	20	10
Cu−15G−15WS_2	70	15	15

2.2 Electrical sliding wear tests

Electrical sliding wear tests were conducted on a self-constructed tribometer with a block-on-ring configuration. The schematic structure of the wear test machine is shown in Fig. 1. The ring was made of Cu−5%Ag alloy with hardness of HB 105, diameter of 320 mm and width of 60 mm. The ring was attached to a high speed spindle which was driven by a 294 kW variable-frequency electrical motor. The samples were loaded against the ring surface by constant-force springs. The sample current was provided by a DC power supply which can provide an electrical current of 0−200 A. A flexible pure copper wire with 0.5 mm^2 cross-sectional area was embedded in each sample at 5 mm from the sliding surface to measure the average contact voltage drop. The schematic diagram for the measurement of contact voltage drops is shown in Fig. 2. The experiments were performed under the ambient conditions at room temperature (15−25 °C) with a relative humidity of 40%−60%. The sliding surfaces of the samples and ring were both polished using 1200 grit abrasive papers and then cleaned with acetone before each test. In all tests, the samples were rubbed against the ring at a velocity of 10 m/s for 5 h under 2.5 N/cm^2 normal pressure with 10 A/cm^2 electrical current. The wear losses of the samples were determined from the mass loss measured by FA2004N electronic analytical balance with 0.1 mg precision before and after each wear test.

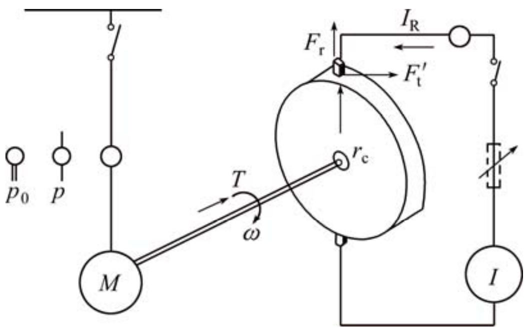

Fig. 1 Schematic diagram of electrical wear test equipment

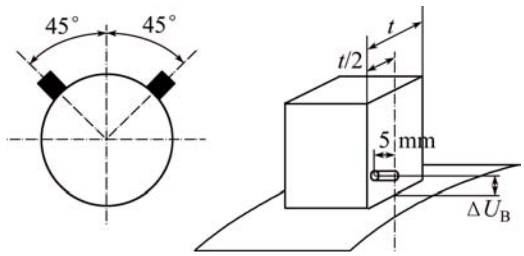

Fig. 2 Schematic diagram of measurement of contact voltage drop

2.3 Detection

The hardness of the composites was evaluated by HBV−30A Brinell Vickers hardness tester at a constant load of 5 kg for 30 s. The density and electrical resistivity of the composites were measured according to Archimedes law and voltmeter−ammeter method. Phase structures of the Cu-based composites were characterized by D/MAX2500V X-ray diffraction (XRD). Microstructures and worn surfaces of the composites were observed by a JSM−6490LV scanning electron microscope (SEM). The equipped energy dispersive X-ray spectroscopy (EDX) apparatus of the SEM system was employed to investigate the element distribution of the composites. The compositions of worn surfaces were analyzed using ESCALAB250 X-ray photoelectron spectroscopy (XPS). These observations were performed without cleaning the worn surfaces in order to obtain information from original features. Surface profile curves of the worn tracks were examined with a YS2205 surface profiler.

3 Results and discussion

3.1 Material characterization

Unlike graphite which has stable chemical properties, WS_2 is unstable at high temperature. It will decompose and react with copper in the hot-pressing process when the sintering temperature exceeds a critical value, which induces marked loss of its lubricity. During the sintering process, the melting copper particles are diffused in the bulk and adhered with each other to form neck regions since WS_2/graphite does not melt with copper. At lower sintering temperature, the adhesion and diffusion between the compacted copper particles do not provide the desired level of mechanical strength for the composites, however, the sintering temperature above 800 °C cause WS_2 to decompose and react with copper. Hence, the sintering temperature for Cu−G−WS_2 dual-lubricant composites is chosen at 800 °C in this work to maintain WS_2 in the bulk and meanwhile obtain the optimum mechanical properties of the composites. Figure 3 shows the X-ray diffraction patterns of the four Cu-based composites after hot-pressing. It is clear that all the characteristic peaks for Cu−G−WS_2 dual-lubricant composites correspond to Cu, graphite and WS_2 and no peaks for other components are detected, indicating that WS_2 does not decompose and no chemical reaction occurs among Cu, graphite and WS_2 during the sintering processes. The copper matrix remains unalloyed, thus, maintains its original mechanical strength and high thermal and electrical conductivity. WS_2 and graphite are completely preserved in the bulk, which guarantee the good wear resistance of the Cu-based composites.

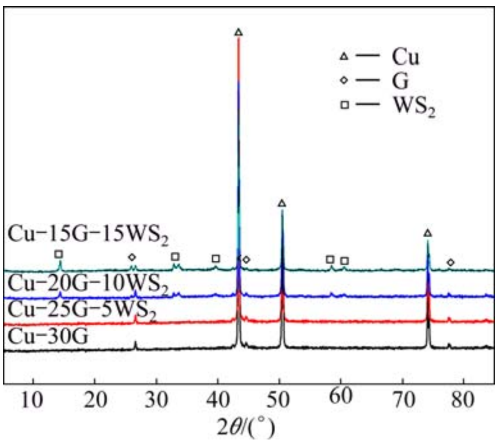

Fig. 3 XRD patterns of sintered Cu-based composites

The typical microstructures of the sintered Cu-based composites are presented in Fig. 4. It can be seen that graphite has thicker black strips while WS_2 has more scrappy strips. The gray matrix is copper. Graphite and WS_2 are distributed uniformly in the copper matrix. No obvious cavities appear at the interface between copper matrix and WS_2/graphite, which reveals a good bonding between the grains in the Cu-based composites. Figure 5 shows the microstructure and corresponding EDX analysis of Cu−15G−15WS_2 composite. It also reveals the morphologies and distributions of graphite and WS_2 in the composite, which further confirm the view above.

The main physical and mechanical properties of the sintered Cu-based composites are listed in Table 2. The relative densities of the composites are all higher than 95%, indicating the dense microstructures of the composites. There is no significant variation that can be observed in relative densities of the three Cu−G−WS_2 composites, while Cu−30G composite exhibits an obviously higher relative density. The higher sintering temperature (900 °C) of Cu−30G composite facilitates adhesion and diffusion between the compacted copper grains, thus favors the formation of sintering necks and decreases the porosity. Because of different densities of copper, graphite and WS_2, the volume content of copper matrix in the composites increases with increasing mass ratio of WS_2 to graphite when the total amount of graphite and WS_2 in mass is fixed. This can be confirmed by increasing the coverage of gray copper matrix from Fig. 4(a) to Fig. 4(d). The electrical conductivities of the Cu-based composites are mainly depended on the volume content of copper in the bulk due to the significant higher electrical conductivity of copper compared with graphite and WS_2. Therefore, the electrical resistivity shows a decreasing tendency when the mass ratio of WS_2 to graphite increases. Theoretically, both graphite and WS_2 are almost soft phases compared with copper, so, the load capacities of the composites are also dominantly determined by the volume content of copper matrix. It is apparent in Table 2 that the Brinell hardness of the composites increases with increasing the mass ratio of WS_2 to graphite.

3.2 Contact voltage drops of composites

Contact voltage drop is one of the main dynamic properties of electrical-rotor system. It is caused by the contact resistance generated at the frictional interface between the sliding pairs when current flows through. Because the surface of solid has a certain degree of roughness, the real contact area between the sliding pairs is only a small fraction of the apparent contact area [12]. When two conductive surfaces are brought into contact, current lines bundle together to pass through separate contact spots between the frictional surfaces named as

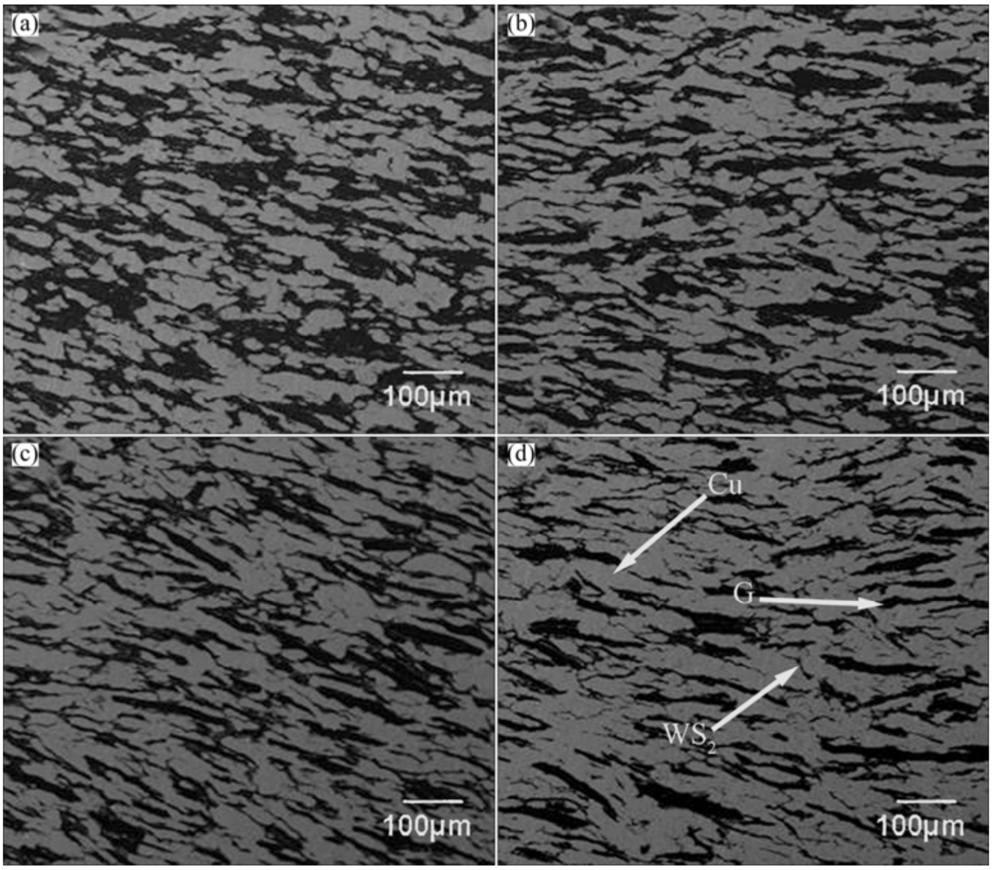

Fig. 4 Typical microstructures of sintered Cu-based composites: (a) Cu−30G; (b) Cu−25G−5WS_2; (c) Cu−20G−10WS_2; (d) Cu−15G−15WS_2

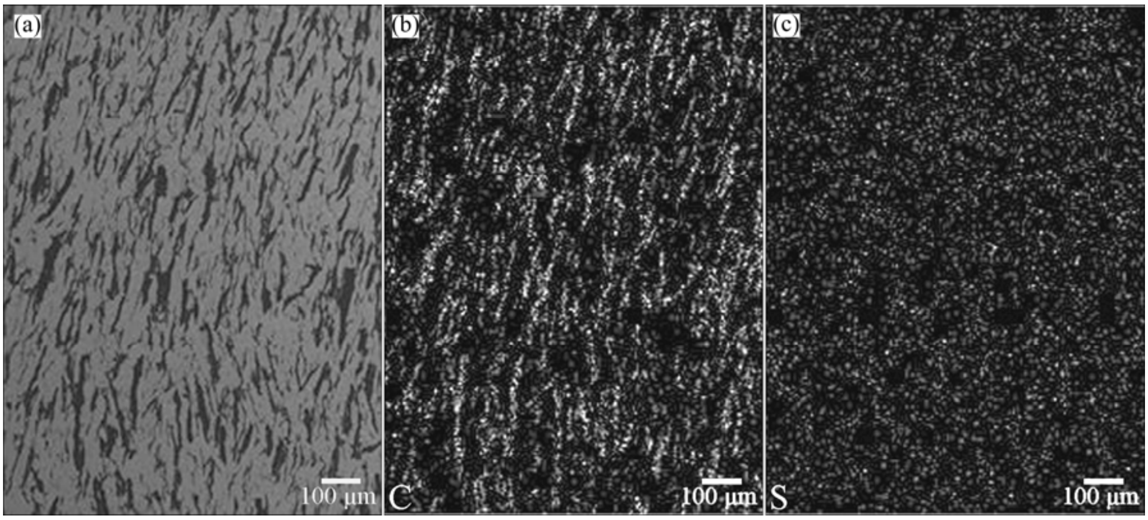

Fig. 5 Microstructure (a) and corresponding EDX maps for carbon (b) and sulfur (c) of sintered Cu−15G−15WS_2 composite

Table 2 Main physical and mechanical properties of sintered Cu-based composites

Sample	Relative density/%	Electrical resistivity/($10^{-7}\Omega\cdot$m)	Hardness (HBS)
Cu−30G	99.16	1.70	26.68
Cu−25G−5WS_2	95.70	1.57	28.02
Cu−20G−10WS_2	95.96	1.38	34.79
Cu−15G−15WS_2	96.23	1.09	42.46

"a-spots". The total electrical conduction area between the sliding pairs is the sum area of all "a-spots", which is only a very small fraction of real contact area [12,26]. Because a tribo-film generally form at the tribo-interface during electrical wear, therefore, the contact resistance consists of the tribo-film resistance and constriction resistance arising from the geometrical effect of current lines from specimen bulk to contact spots.

Figure 6 presents the variations of contact voltage drops of the composites versus sliding time. It can be found that the contact voltage drops of the composites are low in the initial-state and then increase to certain level and remain constant in the steady-state. The stable values in the steady-state are attributed to the formation of tribo-films at the contact interfaces. At the beginning of electrical wear, the tribo-films are not well developed, which cause the samples to directly contact with ring. The contact spots between the samples and ring are mainly metal-metal type, so the contact resistance is constriction resistance. As the wear tests progress, graphite and WS_2 gradually peel off from the matrix and form solid lubricant-rich tribo-films at the contact interfaces between the samples and ring. Figure 7 shows the SEM micrographs of the worn surfaces of the composites after 5 h electrical wear. It is obvious that the tribo-films almost cover the whole worn surfaces of the composites. The formation of metal-metal type contact spots is inhibited and the contact resistance in the steady-state is the sum of constriction resistance and tribo-film resistance, thus causes the increment of contact voltage drops. The contact voltage drops approach a steady-state value when the stable tribo-films form.

It can also be seen from Fig. 6 that the contact voltage drops of the composites increase with increasing

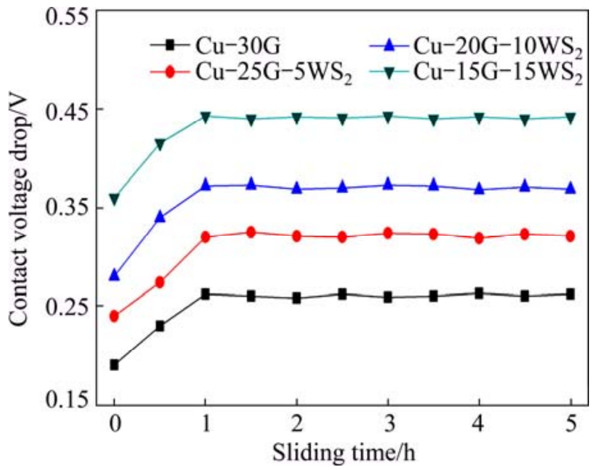

Fig. 6 Contact voltage drop of composites versus sliding time

the mass ratio of WS_2 to graphite. When the mass ratio of WS_2 to graphite increases, the content of WS_2 in the tribo-films increases while the content of graphite decreases. WS_2 is completely insulating while graphite has a certain degree of electrical conductivity, thus hinders the passage of electrical current between the tribo-interfaces and causes the increase of tribo-film resistance. On the other hand, the increasing content of WS_2 in the tribo-films also inhibits the ability of the

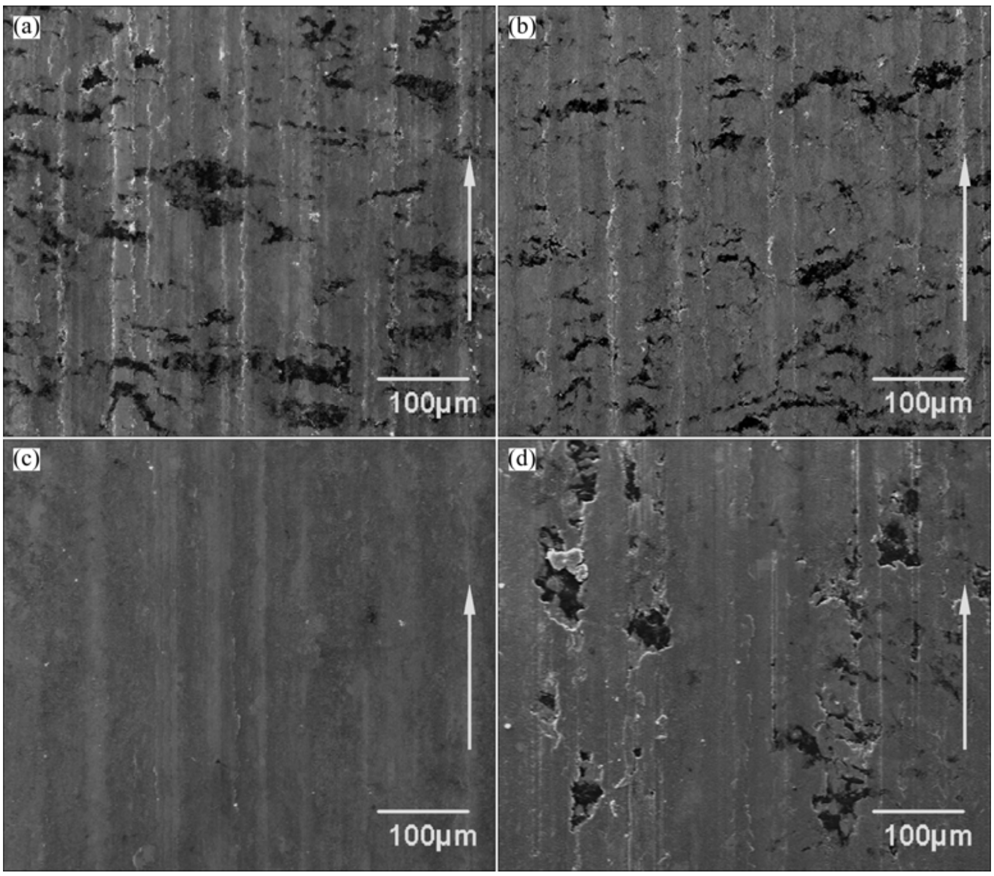

Fig. 7 SEM micrographs of worn surfaces of composites after 5 h electrical wear: (a) Cu−30G; (b) Cu−25G−5WS_2; (c) Cu−20G−10WS_2; (d) Cu−15G−15WS_2 (Arrow indicates sliding direction)

frictional interfaces to form contact spots, which decreases the total electrical conduction area and results in the increment of constriction resistance. Based on the above mentioned analyses, it can be concluded that the tribo-film resistance and constriction resistance both increase when the mass ratio of WS_2 to graphite in the composites increases, which explains the rise of contact voltage drops.

3.3 Wear rates of composites

Wear is also one of the most important characteristics for sliding electrical contacts. The current in sliding contact deforms contact elements, alters friction coefficient, intensifiers wear, and induces damage of rubbing surface [27]. According to Holm's electrical contact theory [28], the total wear of sliding electrical contact materials with an applied electrical current can be divided into three parts: mechanical wear, electrical wear and spark wear. Serious spark induces dramatic increase of both contact voltage drop and wear rate, causing the sample failure and the electrical wear test can not continue. In this work, the contact pressure is sufficient to restrain the emergence of sparks and the SEM micrographs of worn surfaces of the composites also do not show obvious characteristics of spark wear, so, the spark wear can be neglected.

The variations of wear rates of the composites as a function of sliding time are shown in Fig. 8. It can be observed in Fig. 8 that all the wear rates are initially high and then decrease with the increase of sliding time. After the initial-state, the wear rates become stable in the steady-state. In the initial state of sliding, the contact between the samples and ring is metal−metal contact, the adhesions of matrix materials to the ring are easy to occur, thus result in the high wear rates of the composites. With the increase of sliding time, tribo-films gradually form between the rubbing pairs which change the nature of contact from metal−metal to metal−film−metal, thus prevent the direct contact between the counterparts and hinder the adhesions of matrix materials to the ring. For this reason, the wear rates of the composites decrease. The wear rates remain constant when the formation and damage of the tribo-films reach a relatively dynamical equilibrium.

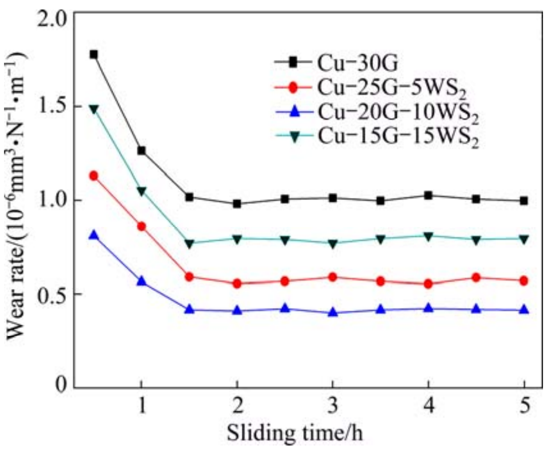

Fig. 8 Wear rates of composites versus sliding time

It can also be found from Fig. 8 that the Cu−20G−10WS_2 composite presents the best wear resistance in the steady-state compared with the other three composites. In the rubbing process, graphite acts as oxygen diffusion barriers at edge and as moisture scavengers in worn areas to reduce WS_2 oxidation, which improves the lubricity of WS_2, thus results in an excellent synergetic lubricating effect. Graphite and WS_2 in Cu−20G−10WS_2 composite gradually peel off from the matrix under the influence of mechanical and electrical loading during electrical sliding to form a continuous and compact tribo-film as shown in Fig. 7(c), which provide adequate lubricating action at the frictional interface and cause dramatic reduction of the wear. When the WS_2 addition in the composites is below 10%, the tribo-films mainly consist of graphite, and the content of WS_2 is not sufficient to form excellent synergetic lubricating action with graphite. The tribo-films are incompact and discontinuous and provide inadequate protection to the samples from the damage by the metal ring. Meanwhile, the worse mechanical strengths of Cu−30G and Cu−25G−5WS_2 composites also cause the hard asperities on the ring surface to press into the sample surface tribo-layers easily, which aggravates the abrasive wear. It is clear in Figs. 7(a) and (b) that the tribo-films of Cu−30G and Cu−25G−5WS_2 composites are obviously destroyed by the plowing and scratching of the metal ring. From Fig. 8, it can also be seen that the wear rate of Cu−15G−15WS_2 composite in the steady-state is significant higher than that of Cu−20G−10WS_2 composite. When the WS_2 addition increases to 20%, the highest contact voltage drop of the composite produces a large amount of Joule heating, which causes a large temperature rise at the frictional interface. The highest interface temperature inhibits the ability of the tribo-film to remain tightly bound to the matrix material and intensifies the adhesion between the sample and ring surface, thus causes spalling of the tribo-film under the contact pressure. From Fig. 7(d), it can be found that the tribo-film of Cu−15G−15WS_2 composite shows obvious mark of spalling. Meanwhile, the highest interface temperature also favors the oxidation of WS_2 in the tribo-film, thus decreases the lubricity of the tribo-film and further increases the wear of Cu−15G−15WS_2 composite. The W 4f XPS spectrum of the worn surface of Cu−15G−15WS_2 composite appears as a triplet which can be fitted into two overlapping doublets as shown in Fig. 9(a). The doublet at lower binding energy originates from WS_2 whereas the other one is consistent with WO_3. By comparing with the W 4f XPS spectrum of pristine WS_2 powder, it can be recognized that the oxidation ratio of WS_2 in the tribo-films of the three Cu−G−WS_2 composites increases with increasing the mass ratio of WS_2 to graphite, as shown in Fig. 9(b). The small amount of graphite in the tribo-film of Cu−15G−15WS_2 composite is not sufficient to act as oxygen diffusion barriers and as moisture scavengers to reduce WS_2 oxidation under the highest interface temperature.

Surface roughness is also an important indicator for the wear performance of the samples. Figure 10 presents the surface profile curves of the worn tracks of the composites after 5 h electrical wear. As shown in Fig. 10, the worn surfaces of the composites turn rough from Cu−20G−10WS_2 to Cu−25G−5WS_2, then Cu−15G−15WS_2 and finally Cu−30G composite, which are consistent with the above mentioned electrical wear performances of the composites. The smoothest worn surface shown in Fig. 10(c) indicates the best wear resistance of the Cu−20G−10WS_2 composite compared with the other three composites.

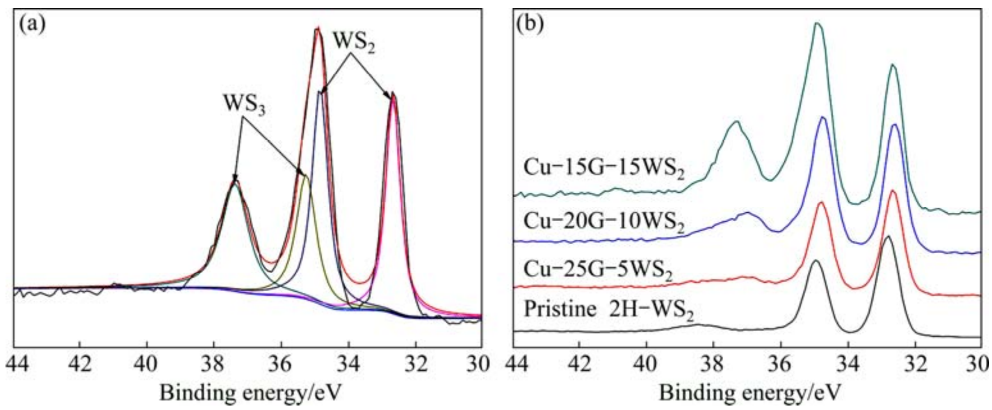

Fig. 9 Fitted W 4f XPS spectrum of worn surface of Cu−15G−15WS_2 composite (a) and superimposed W 4f XPS spectra of pristine WS_2 powder and worn surface of Cu−G−WS_2 composites (b)

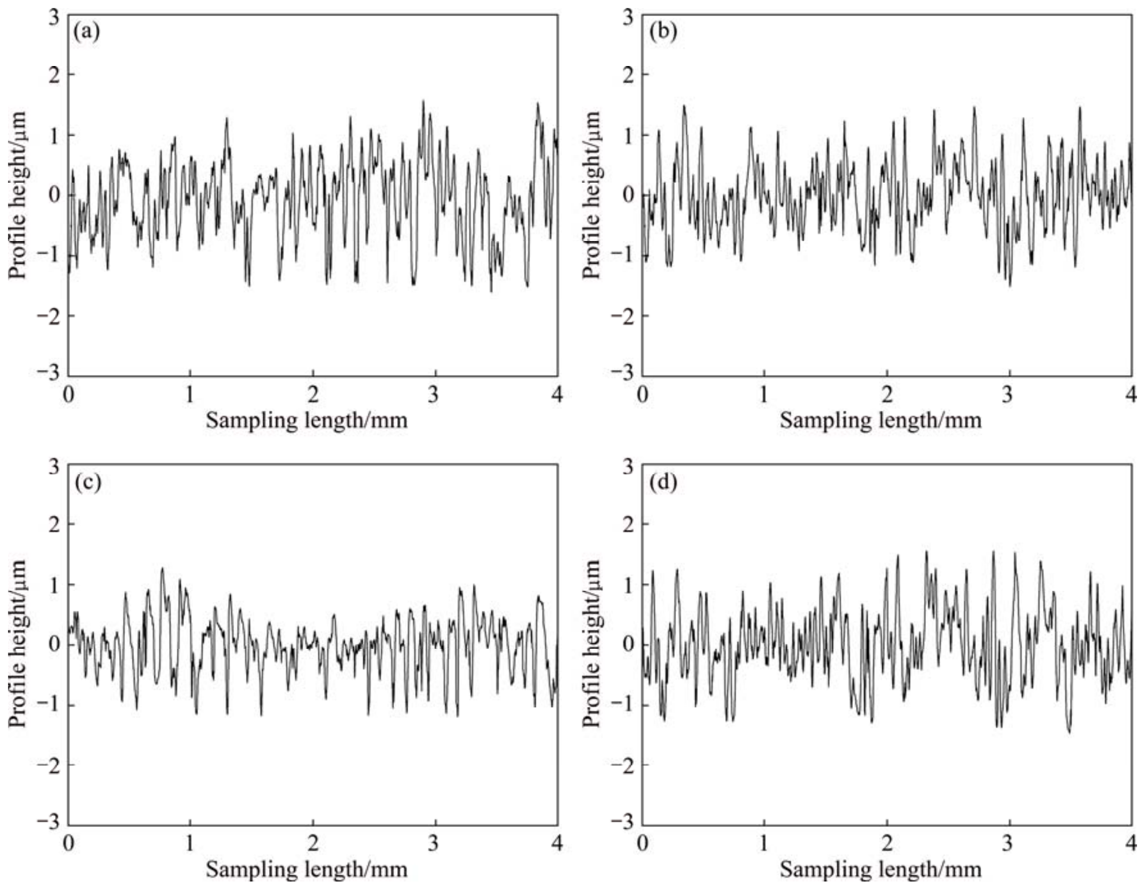

Fig. 10 Surface profile curves of worn tracks of composites after 5 h electrical wear: (a) Cu−30G; (b) Cu−25G−5WS_2; (c) Cu−20G−10WS_2; (d) Cu−15G−15WS_2

4 Conclusions

1) 800 °C is the optimum sintering temperature for Cu−G−WS_2 dual-lubricant composites to obtain the best comprehensive properties of mechanical strength and lubrication performance.

2) Contact voltage drops of the Cu-based composites increase with increasing the mass ratio of WS_2 to graphite.

3) The Cu−20G−10WS_2 composite shows the best wear resistance due to the excellent synergetic lubricating effect of graphite and WS_2.

4) The oxidation rate of WS_2 in the tribo-films of the composites ascends when the mass ratio of WS_2 to graphite increases.

5) The reasonable addition of WS_2 into the Cu−graphite composite can considerably improve the wear resistance without much rise of electrical energy loss.

References

[1] SHIN W G, SONG Y S, SEO Y K. Correlation analysis of brush temperature in brush-type DC motor for predicting motor life [J]. J Mech Sci Technol, 2012, 26(7): 2151−2154.

[2] WANG Y A, LI J X, YAN Y, QIAO L J. Effect of *pv* factor on sliding friction and wear of copper-impregnated metallized carbon [J]. Wear, 2012, 289: 119−123.

[3] SENOUCI A, FRENE C, ZAIDI H. Wear mechanism in graphite−copper electrical sliding contact [J]. Wear, 1999, 225(2): 949−953.

[4] XIE Ming, WANG Song, YANG You-cai, ZHANG Ji-ming, WANG Sai-bei. Electrical sliding wear resistance of Cu−Cr−Y alloy [J]. Heat Treatment of Metals, 2013, 38(9): 82−85. (in Chinese)

[5] WANG Y A, LI J X, YAN Y, QIAO L J. Effect of electrical current on tribological behavior of copper-impregnated metallized carbon against a Cu−Cr−Zr alloy [J]. Tribol Int, 2012, 50: 26−34.

[6] XU Wei, HU Rui, LI Jin-shan, FU Heng-zhi. Effect of electrical current on tribological property of Cu matrix composite reinforced by carbon nanotubes [J]. Transactions of Nonferrous Metals Society of China, 2011, 21(10): 2237−2241.

[7] HU Z L, CHEN Z H, XIA J T, DING G Y. Effect of *PV* factor on the wear of carbon brushes for micromotors [J]. Wear, 2008, 265(3−4): 336−340.

[8] HU Z L, CHEN Z H, XIA J T. Study on surface film in the wear of electrographite brushes against copper commutators for variable current and humidity [J]. Wear, 2008, 264(1−2): 11−17.

[9] HU Zhong-liang, CHEN Zhen-hua, XIA Jin-tong, DING Guo-yun. Wear property of high-resistivity carbon brushes made with and without MoS_2 in variable humidity [J]. Transactions of Nonferrous Metals Society of China, 2008, 18(2): 340−345.

[10] WANG Juan, FENG Yi, LI Shu, LIN Shen. Influence of graphite content on sliding wear characteristics of CNTs−Ag−G electrical contact materials [J]. Transactions of Nonferrous Metals Society of China, 2009, 19(1): 113−118.

[11] HE D H, MANORY R. A novel electrical contact material with improved self-lubrication for railway current collectors [J]. Wear, 2001, 249(7): 626−636.

[12] SLADE P G. Electrical contacts: Principles and applications [M]. New York: Marcel Dekker Inc, 1999.

[13] KAWAKAME M, BRESSAN J D. Study of wear in self-lubricating composites for application in seals of electric motors [J]. J Mater Process Tech, 2006, 179(1−3): 74−80.

[14] MA X C, HE G Q, HE D H, CHEN C S, HU Z F. Sliding wear behavior of copper-graphite composite material for use in Maglev transportation system [J]. Wear, 2008, 265(7−8): 1087−1092.

[15] XU Wei, HU Rui, LI Jin-shan, ZHANG Yong-zhen, FU Heng-zhi. Tribological behavior of CNTs−Cu and graphite−Cu composites with electric current [J]. Transactions of Nonferrous Metals Society of China, 2012, 22(1): 78−84.

[16] CHO K H, HONG U S, LEE K S, JANG H. Tribological properties and electrical signal transmission of copper−graphite composites [J]. Tribol Lett, 2007, 27(3): 301−306.

[17] LÜ Le-hua, SUN Le-min, SHANGGUAN Bao, ZHANG Yong-zhen. Effects of graphite content on current carrying friction and wear behaviors of graphite/copper composites [J]. Lubrication Engineering, 2013, 38(1): 24−27. (in Chinese)

[18] XIAN G J, WALTER R, HAUPERT F. A synergistic effect of nano-TiO_2 and graphite on the tribological performance of epoxy matrix composites [J]. J Appl Polym Sci, 2006, 102(3): 2391−2400.

[19] LI J L, XIONG D S. Tribological properties of nickel-based self-lubricating composite at elevated temperature and counterface material selection [J]. Wear, 2008, 265(3−4): 533−539.

[20] HU K H, HUANG F, HU X G, XU Y F, ZHOU Y Q. Synergistic effect of nano-MoS_2 and anatase nano-TiO_2 on the lubrication properties of MoS_2/TiO_2 nano-clusters [J]. Tribol Lett, 2011, 43(1): 77−87.

[21] LI X B, GAO Y M, XING J D, WANG Y, FANG L. Wear reduction mechanism of graphite and MoS_2 in epoxy composites [J]. Wear, 2004, 257(3−4): 279−283.

[22] GARDOS M N. The synergistic effects of graphite on the friction and wear of MoS_2 films in air [J]. Tribol T, 1988, 31(2): 214−227.

[23] GREENBERG R, HALPERIN G, ETSION I, TENNE R. The effect of WS_2 nanoparticles on friction reduction in various lubrication regimes [J]. Tribol Lett, 2004, 17(2): 179−186.

[24] SCHARF T W, RAJENDRAN A, BANERJEE R, SEQUEDA F. Growth, structure and friction behavior of titanium doped tungsten disulphide (Ti−WS_2) nanocomposite thin films [J]. Thin Solid Films, 2009, 517(19): 5666−5675.

[25] VADIRAJ A, KAMARAJ M. Comparative wear behavior of MoS_2 and WS_2 coating on plasma-nitrided SG iron [J]. J Mater Eng Perform, 2010, 19(2): 166−170.

[26] KOGUT L. Electrical performance of contaminated rough surfaces in contact [J]. J Appl Phys, 2005, 97(10):103723−103727.

[27] KONCHITS V V, KIM C K. Electric current passage and interface heating [J]. Wear, 1999, 232(1): 31−40.

[28] HOLM R. Electric contacts theory and applications [M]. Berlin: Springer, 1967.

二硫化钨含量对铜−石墨−二硫化钨复合材料电滑动磨损性能的影响

钱 刚，凤 仪，陈阳明，莫 飞，王雨晴，刘文宏

合肥工业大学 材料科学与工程学院，合肥 230009

摘 要：采用粉末冶金热压法制备了 4 种以石墨和二硫化钨为润滑剂的铜基复合材料，并采用环−块式磨损机对复合材料与 Cu−5%银合金环对磨时的电滑动磨损性能进行测试。结果表明，铜−石墨−二硫化钨双润滑剂复合材料在 800 °C 烧结时可以在保证其良好的润滑性能的同时获得较优的力学性能。随着二硫化钨与石墨质量比的增加，复合材料的接触电压降增加，铜−20%石墨−10%二硫化钨复合材料在电磨损过程中显示出最佳的抗磨性能，这主要是由于石墨和二硫化钨之间优异的协同润滑作用。在铜−石墨复合材料中添加适量的二硫化钨可以在电能损耗增加不多的同时显著提高其磨损抗力，为制备高性能滑动电接触材料提供了一种新颖的设计思路。

关键词：铜基复合材料；石墨；二硫化钨；协同润滑；磨损率；接触电压降

(Edited by Yun-bin HE)